Korean J. Chem. Eng., 39(5), 1333-1338 (2022)
DOI: 10.1007/s11814-021-0980-4

pISSN: 0256-1115
eISSN: 1975-7220

Electrode modifier performance of TiO_2 incorporated carbon quantum dots nanocomposites on $Fe(CN)_6^{3-}/Fe(CN)_6^{4-}$ electrochemical system

Zul Arham*,† and Kurniawan Kurniawan**

*Department of Mathematics and Natural Sciences, Faculty of Tarbiyah, Institut Agama Islam Negeri (IAIN) Kendari, 93116, Southeast Sulawesi, Indonesia
**Department of Textile Chemistry, Politeknik STTT Bandung, 40272, West Java, Indonesia
(*Received 19 August 2021 • Revised 19 September 2021 • Accepted 13 October 2021*)

Abstract−TiO_2 incorporated carbon quantum dot nanocomposite, (CQDs@TiO_2) was synthesized and applied as a new modifier for carbon paste electrode (CPE). The synthesis process consisted of two steps: the synthesis of a carbon quantum dot (CQDs) solution electrochemically and the synthesis of CQDs@TiO_2 by impregnation. The characterization results show that the morphology of CQDs@TiO_2 is composed of small particles with different particle sizes which causes the nanocomposite surface to be non-uniform. The impregnation process causes a change in the average particle size of TiO_2 from 29.32 to 33.23 nm. This process also produces new diffractograms at positions 2θ=53.75° and 54.95°. In addition, its process changes the specific wave number absorption ($1/\lambda$) TiO_2 for -OH stretching (3,300 cm^{-1} to 3,369 cm^{-1}) and -OH bending (1,631 cm^{-1} to 1,660 cm^{-1}). This shift in wavenumber was followed by the presence of new absorption at wavenumbers of 2,162 cm^{-1} and 1,371 cm^{-1}. Based on the performance test of CQDs@TiO_2 as a CPE modifier, it shows that CQDs@TiO_2 improves CPE performance in the $Fe(CN)_6^{3-}/Fe(CN)_6^{4-}$ solution system. It is characterized by an increase in both oxide and reducing currents and a narrowing of the voltammogram peaks. The optimum mass of CQDs@TiO_2 as a CPE modifier is 0.01 g with an electroactive surface area of 0.27 cm^2. The overall results of this work indicate that the CQDs@TiO_2 nanocomposite can be applied as an electrode modifier for electrochemical sensor applications in the future.

Keywords: New Modifier, CQDs@TiO_2 Nanocomposite, CPE, $Fe(CN)_6^{3-}/Fe(CN)_6^{4-}$

INTRODUCTION

In recent years, the improvement of electrode performance in the electrometric analysis of chemical compounds has involved modifying the working electrode [1-3]. This electrode plays a role in providing information about the nature and amount of the analyte. This basis is the reason for designing a working electrode that is stable and capable of detecting an analyte at trace concentration. The mechanism of working electrode modification is carried out using a modifier, both organic modifiers such as 1H-1, 2, 4-triazole-3-thiol [4], inorganic such as zinc oxide [5], as well as a combination of modifiers such as TiO_2-Ionophores BEK6 [6]. The modification makes the electron transfer between a working electrode and the analyte faster, so that the redox current increases. This has an impact on the performance of the working electrode, such as increased sensitivity, lower detection limit, and more selective analysis.

Carbon paste electrode (CPE) is a working electrode that is widely applied in electrometric-based analysis. The selection is based on several considerations, such as easy to update and modify, economical, very low current interference, and instrument design that can be made in small sizes. These advantages make the use of CPE very wide. For example, CPE is used in developing an analysis using voltammetry techniques [7-9], amperometry [10-14], and potentiometry [15-19]. However, without modification, CPE is reported to have some drawbacks, such as a wide current peak. This makes it difficult to determine the current and redox potential of the analyte. So researchers have tried to make modifications to the CPE.

The choice of method in the preparation of a modifier becomes an important parameter to reort. In general, the criteria for the method used are easy to apply, simple steps and equipment, and a short synthesis process. In preparing a modifier, the use of inorganic materials is an interesting study. This is based on the use of organic material as a modifier which has a long process of processing. In addition to the inorganic modifiers previously mentioned, other modifiers reported include ZnO/RuO_2 nanoparticles [20], ZnO/CdO/SnO_2 nanocomposites [21], and CuO doped CeO_2 nanocomposites [22]. These modifiers have been applied to various types of working electrodes. Specifically for CPE, some of the modifiers that have been reported include TiO_2 [23], multi-walled carbon nanotubes [24], zeolite [25], and CuO/g-C_3N_4 composite [26].

Based on the problems above, this study reports on the electrochemical performance of CQDs@TiO_2 nanocomposite as a CPE modifier. The modifiers reported are two semiconductor materials incorporated through the impregnation process. The TiO_2 semiconductor has been reported for its performance as a CPE modifier in various analyses, such as Pb^{2+} ion [27], cypermethrin pesticide [23], clozapine [28], gallic acid [29], benserazide [30], anti-Parkin-

†To whom correspondence should be addressed.
E-mail: arhamzul88@yahoo.com

son drug pramipexole [31], and other applications. The choice of TiO_2 as a modifier was due to the good surface area and adsorption capacity of the analyte. In sensor applications, TiO_2 has good biocompatibility properties. The electrocatalytic performance of TiO_2 will increase when modified. Modification with CQDs will produce nanocomposite with unique hybrid structures. Although the use of CQDs as modifier in the development of electrometric analysis has not been specifically reported, however, since Xu et al. in 2004 reported their findings, CQDs have attracted the attention of researchers in various fields [32,33]. CQDs have a unique surface area with nanoscale particle size. This condition is supported by strong chemical properties and good biocompatibility [34]. The incorporation process of the two is expected to produce a modifier with good electrochemical performance. In this work, electrochemical performance studies were conducted in the $Fe(CN)_6^{3-}/Fe(CN)_6^{4-}$ solution system. This system is commonly used in studying the electrochemical response of a new working electrode [35,36]. In addition to the stable nature of the solution, this system has clear redox properties with a reversible reaction.

MATERIALS AND METHODS

1. Synthesis of CQDs and TiO_2 Nanoparticle

CQDs were synthesized using an electrochemical method through work modification reported by [37]. Two graphite rods with a diameter of 0.5 cm were placed in an electrochemical cell containing a mixed solution of ethanol and distilled water (20 : 1) with the addition of 0.40 g sodium hydroxide. The graphite rods were placed as anode and cathode with a distance of 3.5 cm. The synthesis process was carried out for five hours with a potential bias of 12.0 V.

The TiO_2 nanoparticle was synthesized using the sol gel method with titanium tetra isopropoxide (TTIP) as the precursor [38]. Into a reflux flask (containing 4 mL of TTIP, 0.5 mL of acetylacetonate and 15 mL of ethanol) were successively added 15 mL of ethanol, 2 mL of distilled water, and 1 mL of 0.5 M acetic acid. Next, the mixture was refluxed for three hours at 50 °C and followed by stirring using a magnetic stirrer for one hour. The TiO_2 sol gel formed was evaporated at room temperature for 48 hours, then heated at 100 °C and calcined for three hours at 500 °C.

2. Synthesis of CQDs@TiO_2

A total of 4 mL of CQDs was added to a mixture of 20 mL of distilled water and 6 mL of ethanol. This composition refers to the work reported by [37]. The solution mixture was homogenized using a magnetic stirrer and 0.4 g of TiO_2 nanoparticle was added slowly. To produce a good homogeneous suspension, the mixture was stirred for four hours at room temperature. The resulting suspension was transferred in a container and heated at 140 °C for four hours. The formed CQDs@TiO_2 was separated and washed three times using distilled water and dried at 40 °C for 24 hours. Furthermore, it was characterized using SEM, XRD, and FTIR-ATR.

3. Electrochemical Performance of CQDs@TiO_2 Modifier

The electrochemical performance of CQDs@TiO_2 was studied by cyclic voltammetry technique using a three-electrode-based potentiostat DY-2100B. Carbon paste electrode with the addition of CQDs@TiO_2 (CPE/CQDs@TiO_2) was used as the working electrode. The Ag/AgCl was used as the reference electrode. Pt wire was used as auxiliary electrode. Measurements were carried out in 0.001 M $K_3[Fe(CN)_6]$ analyte solution with 0.1 M sodium chloride supporting electrolyte. The potential range used was −0.8 V to +0.8 V.

The working electrode was prepared by weighing the CQDs@TiO_2 nanocomposite as much as 0.01 g, 0.03 g and 0.05 g. Each mass was mixed with 0.70 g graphite powder and 0.30 paraffin oil in a vial. Then homogenized at a temperature of 80 °C using a magnetic stirrer. The paste formed was then put into a glass tube with a diameter of 3 mm and connected with copper wire to provide current during electrochemical measurements. For comparison, CPE without modifier was prepared following the procedure we previously reported [23]. In summary, graphite powder and paraffin oil were mixed in a ratio of 7 : 3 and mechanically homogenized at 80 °C.

RESULTS AND DISCUSSION

1. Characterization of SEM, XRD, and FTIR

Fig. 1 shows the SEM characterization of TiO_2 nanoparticle and CQDs@TiO_2 nanocomposite. The two materials have different surface shapes. TiO_2 nanoparticle (Fig. 1[A]) is composed of particles of various sizes, which causes their surface to become irregular. In addition, the pore structure of TiO_2 looks tight. Although the particle size varies, in general the TiO_2 particle is homogeneously arranged. Unlike the case with TiO_2 nanoparticle, the surface of CQDs@TiO_2 (Fig. 1[B]) is composed of small grains with different particle sizes.

The crystal size of CQDs@TiO_2 nanocomposite was studied using XRD by comparing it to the crystal size of TiO_2 nanoparticle. Based on Fig. 2, there are differences in the diffractogram peaks between TiO_2 nanoparticle (black line) and CQDs@TiO_2 nanocomposite (red line).

The incorporation of CQDs@TiO_2 nanocomposite produced new diffractogram peaks at positions 2θ=53.75°, 54.95°, 70.03°, and 78.48°. This shows the success of the synthesis process by impregnation for the modifier. The success of the incorporation was confirmed by the change in the average particle size of the nanocomposite. Based on the Scherrer equation, CQDs@TiO_2 has a larger particle size than TiO_2, where the average particle size of TiO_2 and CQDs@TiO_2 are 29.32 nm and 33.23 nm, respectively. The change in the average particle size assumes that the CQDs are distributed on the TiO_2 surface. This phenomenon is corroborated by the SEM

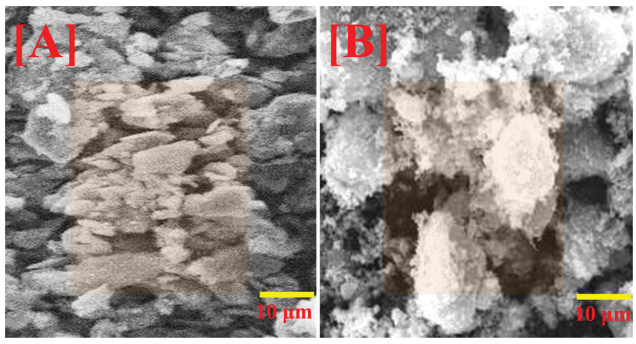

Fig. 1. Characterization of SEM: [A] TiO_2 nanoparticle; [B] CQDs@TiO_2 nanocomposite.

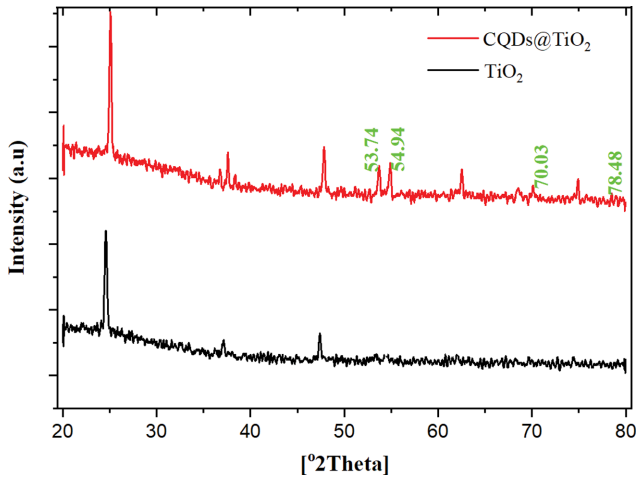

Fig. 2. Characterization of XRD: TiO_2 nanoparticle (black line); CQDs@TiO_2 nanocomposite (red line).

Table 1. Data comparison of °2Theta and d-spacing from TiO_2 nanoparticle and CQDs@TiO_2

Materials	Pos [°2theta]	d-Spacing (nm)
TiO_2 nanoparticle	24.56	0.36
	37.07	0.24
	47.39	0.19
	62.07	0.14
	67.19	0.13
	74.38	0.12
CQDs@TiO_2	25.09	0.35
	37.60	0.23
	47.86	0.18
	53.75	0.17
	54.94	0.16
	62.52	0.14
	70.03	0.13
	74.90	0.12
	78.48	0.12
	79.05	0.12

characterization in Fig. 1. In addition, the comparison to standard carbon (Ref. code: 00-008-0415) confirms the information that the new diffractogram produced is from carbon particles. From the literature comparison, it was concluded that the CQDs particles were distributed on the surface of the TiO_2 pores. This is confirmed by the absence of a specific diffractogram of the CQDs reported to be at position 2θ=26°, where this position is the amorphous phase for carbon [39]. The °2theta and d-spacing data of TiO_2 nanoparticle and CQDs@TiO_2 are shown in Table 1.

The success of the synthesis process was also confirmed by the results of the FTIR-ATR characterization (Fig. 3). As with SEM and XRD characterization, FTIR-ATR characterization was also carried out on TiO_2 nanoparticles (black line) and CQDs@TiO_2 nanocomposite (red line). In general, the FTIR-ATR characterization results show that the incorporation of CQDs causes a shift in the

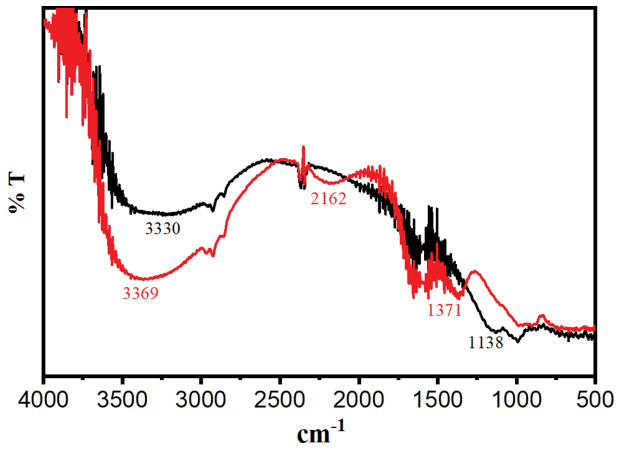

Fig. 3. Characterization of FTIR-ATR: TiO_2 nanoparticle (black line); CQDs@TiO_2 nanocomposite (red line).

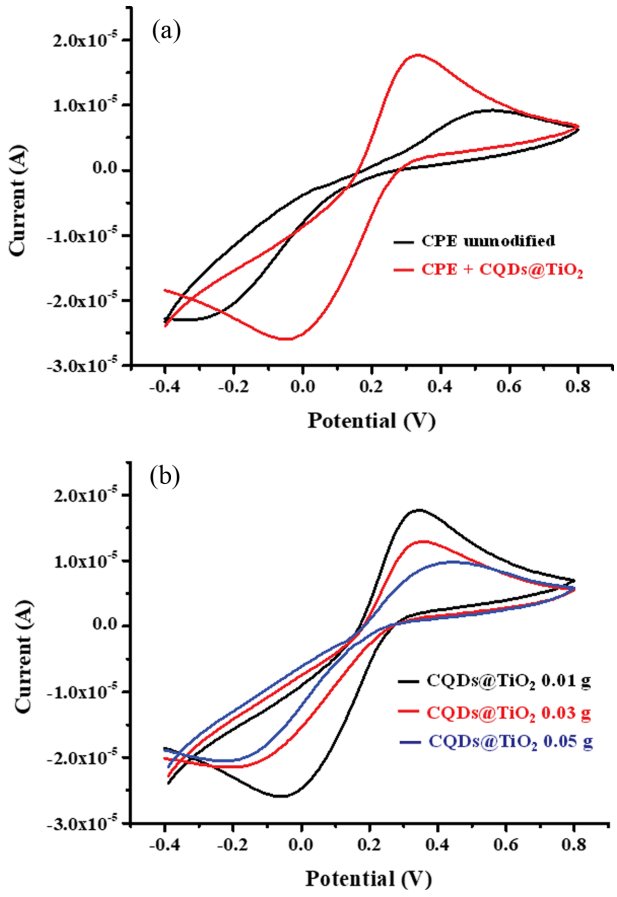

Fig. 4. (a) Cyclic voltammograms of CPE unmodified and CPE/CQDs@TiO_2; (b) effect of mass CQDs@TiO_2 on cyclic voltammogram current.

wavenumber (cm^{-1}) of the TiO_2 nanoparticles. Specific IR absorption for TiO_2 is seen at wave numbers 3,300 cm^{-1} and 1,631 cm^{-1} which are -OH stretching and -OH bending absorption from water absorption on the TiO_2 surface, respectively [40]. The shift of TiO_2-specific IR absorption intensity towards higher wave numbers

Table 2. Comparison of current and potential values of CPE and CPE/CQDs@TiO_2 in $Fe(CN)_6^{3-}/Fe(CN)_6^{4-}$ solution system

Type of electrode	Ip_a (μA)	Ip_c (μA)	Ep_a (V)	Ep_c (V)
CPE	4.14	−0.17	0.53	−0.3
CPE/CQDs@TiO_2	15.46	−14.41	0.33	−0.05

(3,369 cm^{-1} and 1,660 cm^{-1}) indicates the formation of bond interactions between CQDs and TiO_2 on the nanocomposite surface. This formation was confirmed by the emergence of new absorptions at wave numbers 2,162 cm^{-1} and 1,371 cm^{-1}. This absorption is proposed as a specific IR absorption for CQDs@TiO_2 nanocomposite. The reference approximation shows that the two wavenumbers come from the triatomic molecule O=C=O [41]. In addition, the fingerprint area also shows a decrease in intensity at the wave number of 992 cm^{-1}. This wave number comes from the Ti=O stretching absorption.

2. Electrochemical Performance

Fig. 4(a) shows a cyclic voltammogram of two working electrodes, CPE unmodification (black line) and CPE modified CQDs@TiO_2 (red line) in the $Fe(CN)_6^{3-}/Fe(CN)_6^{4-}$ solution system. CPE is used as a comparison to determine the effect of the CQDs@TiO_2 modifier, while the use of $Fe(CN)_6^{3-}/Fe(CN)_6^{4-}$ solution is based on the stability of the solution and the clarity in the number of electrons transferred when the redox reaction occurs [23]. Based on Fig. 4(a), the CPE produces a wide voltammogram peak with a small redox current. These results indicate that electron transfer is slow. This is corroborated by the values of oxidation (E_a) and reduction (E_c) potentials of 0.53 V and −0.30 V, respectively. The widening of the voltammogram peaks will reduce the accuracy in determining the current values for both oxidation and reduction. The addition of CQDs@TiO_2 as a modifier improves the electrochemical performance of CPE. CQDs@TiO_2 accelerated electron transfer and increased peak currents, both oxidation and reduction (Table 2). The addition of CQDs@TiO_2 also causes the peak current to narrow. The increase in electron transfer rate could be due to the high conductivity of TiO_2 anatase [31] and the increased surface-volume ratio of the carbon paste [42]. Based on the comparison of anodic (Ip_a) and cathodic (Ip_c) peak currents, it is stated that the reaction that occurs in the $Fe(CN)_6^{3-}/Fe(CN)_6^{4-}$ system for CPE is irreversible, with the value of $Ip_a/Ip_c \neq 1$. Meanwhile, with the addition of reaction modifier CQDs@TiO_2 is reversible, with a value of $Ip_a/Ip_c=1$. However, based on the difference in anodic and cathodic potentials (ΔE_p) it is known that both CPE and CPE/CQDs@TiO_2 in the $Fe(CN)_6^{3-}/Fe(CN)_6^{4-}$ is not Nertsian.

Fig. 4(b) shows the effect of mass CQDs@TiO_2 which is used as a modifier. The addition of CQDs@TiO_2 in excess will decrease the oxidation and reduction currents. In addition, the oxidation potential becomes more positive while the reduction potential becomes more negative. The addition of 0.01 g of CQDs@TiO_2 (black line) resulted in higher currents for both oxidation and reduction than the addition of 0.03 g (red line) and 0.05 g (blue line) CQDs@TiO_2. Excess CQDs@TiO_2 will cause a decrease in electrode homogeneity, slow electron transfer, and a decrease in peak current.

3. Estimation of Electroactive Surface Area

Based on the scan rate variation (Fig. 5(a)), it shows a linear relationship between the current and the potential scan rate for CPE/CQDs@TiO_2, where the greater the potential scan rate, the higher the current generated (Table 3). This situation explains that the interaction of $Fe(CN)_6^{3-}/Fe(CN)_6^{4-}$ on the electrode surface is controlled by the diffusion process.

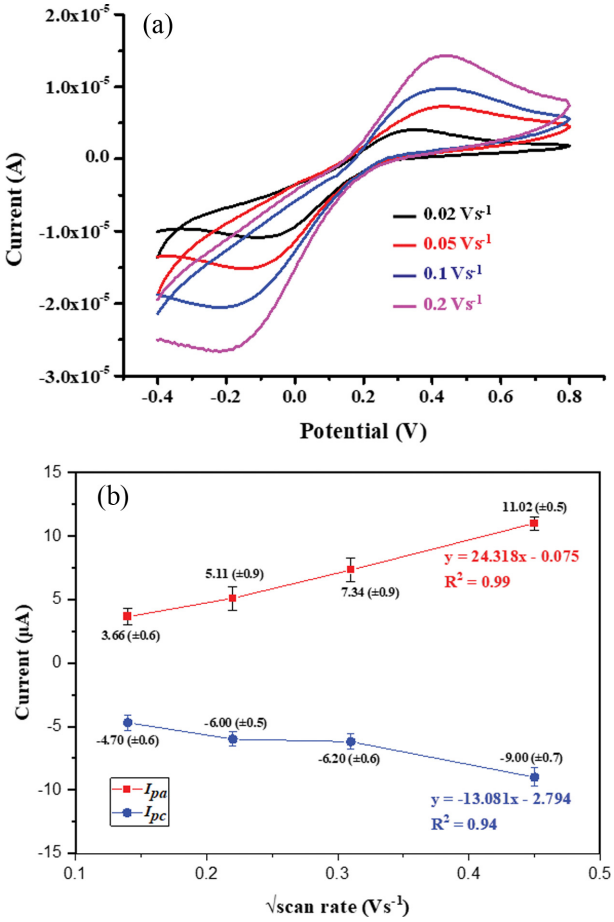

Fig. 5. (a) Cyclic voltammogram of various scan rates CPE/CQDs@TiO_2; (b) Plot anodic peak current vs root scan rate.

Table 3. Effect of scan rate on the electrochemical performance of CPE/CQDs@TiO_2

Scan rate (V/s)	Ip_a (μA)	Ip_c (μA)	Ep_a (V)	Ep_c (V)
0.02	3.66	−4.74	0.34	−0.10
0.05	5.11	−5.97	0.42	−0.12
0.1	7.34	−6.14	0.43	−0.19
0.2	11.02	−8.95	0.43	−0.20

The slope value of the anodic peak current vs scan rate plot (Fig. 5(b)) was used to estimate the electroactive surface area of CPE/CQDs@TiO_2. The determination is carried out using the Randles-Sevcik equation [43-45]. The calculation results show that the electrochemically active surface area (EASA) of the electrode is 0.27 cm^2. Our reported surface area is smaller than the CPE modification reported by [31,43], but larger than that reported by [46]. The values for both are 0.39 cm^2 and 0.15 cm^2, respectively. The incorporation between CQDs and TiO_2 makes the electron transfer at

the electrode surface fast. It shows high electrochemical performance. Another unique phenomenon of this incorporation process is the reduction in the electroactive surface area of the CPE. Based on the calculation of the EASA value, pristine CPE has an EASA value of 0.39 cm^2. This value is consistent with the pore properties of the pristine CPE matrix.

CONCLUSIONS

The presence of new modifiers, such as CQDs@TiO_2 nanocomposite, has become an important point in the development of electrometric analysis methods for chemical compounds. The modifier will increase the redox current on the surface of the working electrode. This has implications for the performance of the working electrode which is more sensitive and selective in detecting analytes. Incorporation of CQD with TiO_2 by impregnation has succeeded in increasing the redox property of CPE. In the presence of CQDs@TiO_2, the current response, both oxidation (Ip_a) and reduction (Ip_c) of CPE were significantly increased in the $Fe(CN)_6^{3-}/Fe(CN)_6^{4-}$ solution system. Not only that, the modifier was also effective in increasing the electron transfer rate between the electrode surface and the bulk solution. The testing results of the mass modifier, increase in redox current and electron transfer rate are influenced by the use of mass modifier. In this case, we report the use of CQDs@TiO_2 mass of 0.01 g as the best mass to improve CPE performance. However, further testing of the performance of the CQDs@TiO_2 modifier needs to be done in the future. This test is concerned with the effect of potential bias on the characteristics of CQDs. In addition, the performance of the CQDs@TiO_2 modifier with TiO_2 nanoparticle needs to be compared and studied.

DECLARATIONS

Conflict of Interest

Zul Arham declares that she has no conflict of interest. Kurniawan declares that he has no conflict of interest.

Ethics Approval

This study does not contain experiments that involve humans or animals other than the authors who performed the work.

Informed Consent

Not applicable.

REFERENCES

1. M. Nurdin, L. Agusu, A. A. M. Putra, M. Maulidiyah, Z. Arham, D. Wibowo, M. Z. Muzakkar and A. A. Umar, *J. Phys. Chem. Solids.*, **131**, 104 (2019).
2. M. Nurdin, O. A. Prabowo, Z. Arham, D. Wibowo, M. Maulidiyah, S. K. M. Saad and A. A. Umar, *Surf. Interfaces*, **16**, 108 (2019).
3. M. Nurdin, Z. Arham, S. Rahayu and M. Maulidiyah, *J. Rekayasa Kim. Lingkung*, **15**, 71 (2020).
4. Z. Danyıldız, D. Uzun, T. T. Calam and E. Hasdemir, *J. Electroanal. Chem.*, **805**, 177 (2017).
5. L. U. Yuan-Yuan, C. Meng-Ni, G. A. O. Yi-Li, Y. Jian-Mao, M. A. Xiao-Yu and L. I. U. Jian-Yun, *Chin. J. Anal. Chem.*, **43**, 1395 (2015).
6. M. Nurdin, N. Dali, I. Irwan, M. Maulidiyah, Z. Arham, R. Ruslan, B. Hamzah, S. Sarjuna and D. Wibowo, *Anal. Bioanal. Electrochem.*, **10**, 1538 (2018).
7. M. Nurdin, Z. Arham, J. Rasyid, M. Maulidiyah, F. Mustapa, H. Sosidi, R. Ruslan and L. O. A. Salim, *Electrochemical performance of carbon paste electrode modified TiO_2/Ag-Li (CPE-TiO_2/Ag-Li) in determining fipronil compound*, in: J. Phys. Conf. Ser., IOP Publishing, 12067 (2021).
8. A. Abdulaziz Nabil, K. Emran and H. Alanazi, *Turkish J. Chem.*, **44**, 1122 (2020).
9. G. Fadillah, S. Triana, U. Chasanah and T. A. Saleh, *Sens. Bio-Sensing Res.*, **30**, 100391 (2020).
10. G. Manasa, C. Raj, A. K. Satpati and R. J. Mascarenhas, *Electroanalysis*, **32**, 2431 (2020).
11. A. R. de Brito, N. dos Santos Reis, P. C. Oliveira, D. V. B. Rezende, G. P. Monteiro, G. A. Soares, R. S. de Jesus, A. S. Santos, L. C. Salay and J. R. de Oliveira, *J. Food Sci. Technol.*, **57**, 1342 (2020).
12. A. Wong, A. M. Santos, O. Fatibello-Filho and M. D. P. T. Sotomayor, *Electroanalysis*, **33**, 431 (2021).
13. N. Nontawong, M. Amatatongchai, P. Jarujamrus, D. Nacapricha and P. A. Lieberzeit, *Sensors Actuators B Chem.*, **334**, 129636 (2021).
14. H. L. Tcheumi, A. P. Kameni Wendji, I. K. Tonle and E. Ngameni, *J. Anal. Methods Chem.*, 2020 (2020).
15. M. A. Zayed, W. H. Mahmoud, A. A. Abbas, A. E. Ali and G. G. Mohamed, *RSC Adv.*, **10**, 17552 (2020).
16. J. Radić, M. Buljac, B. Genorio, E. Gričar and M. Kolar, *Sensors*, **21**, 2955 (2021).
17. M. A. Zayed, A. A. Abbas, W. H. Mahmoud, A. E. Ali and G. G. Mohamed, *Microchem. J.*, **159**, 105478 (2020).
18. N. Rajabi, M. Masrournia and M. Abedi, *Chem. Methodol.*, **4**, 660 (2020).
19. A. M. Abdel-Raoof, A. Elsonbaty, S. Abdulwahab, W. S. Hassan and M. S. Eissa, *Microchem. J.*, **165**, 106185 (2021).
20. M. T. Uddin, M. M. Alam, A. M. Asiri, M. M. Rahman, T. Toupance and M. A. Islam, *RSC Adv.*, **10**, 122 (2020).
21. M. M. Alam, A. M. Asiri, M. M. Rahman and M. A. Islam, *Surf. Interfaces*, **19**, 100540 (2020).
22. M. M. Alam, M. M. Rahman, A. M. Asiri and M. A. Fazal, *J. Mater. Sci. Mater. Electron.*, **32**, 5259 (2021).
23. M. Nurdin, M. Maulidiyah, M. Z. Muzakkar and A. A. Umar, *Microchem. J.*, **145**, 756 (2019).
24. A. Afkhami, H. Ghaedi, T. Madrakian and M. Rezaeivala, *Electrochim. Acta.*, **89**, 377 (2013).
25. M. Khasanah, A. A. Widati, U. S. Handajani, M. R. Shofiyyah, S. A. Rakhma and H. Predianto, *Imprinted zeolite modified carbon paste electrode as a selective potentiometric sensor for blood glucose*, in: AIP Conf. Proc., AIP Publishing LLC, 20011 (2020).
26. K. Atacan and M. Özacar, *Mater. Chem. Phys.*, **266**, 124527 (2021).
27. N. Belkhamsa, L. Ouattara and M. Ksibi, *J. Electrochem. Soc.*, **162**, B212 (2015).
28. M. H. Mashhadizadeh and E. Afshar, *Electrochim. Acta.*, **87**, 816 (2013).
29. J. Tashkhourian, S. F. N. Ana, S. Hashemnia and M. R. Hormozi-Nezhad, *J. Solid State Electrochem.*, **17**, 157 (2013).
30. A. A. Ensafi, H. Bahrami, B. Rezaei and H. Karimi-Maleh, *Mater.*

Sci. Eng. C., **33**, 831 (2013).
31. S. K. Hassaninejad-Darzi and F. Shajie, *J. Braz. Chem. Soc*., **28**, 529 (2017).
32. Q. Hu, X. Gong, L. Liu and M. M. F. Choi, *J. Nanomater*., 2017 (2017).
33. A. Pal, M. P. Sk and A. Chattopadhyay, *Mater. Adv*., **1**, 525 (2020).
34. T. K. Mondal, A. Gupta, B. K. Shaw, S. Mondal, U. K. Ghorai and S. K. Saha, *RSC Adv*., **6**, 59927 (2016).
35. K. Atacan, *J. Alloys Compd*., **791**, 391 (2019).
36. S. Z. Bas, N. Yuncu, K. Atacan and M. Ozmen, *Electrochim. Acta*., **386**, 138519 (2021).
37. L. Sang, J. Lin and Y. Zhao, *Int. J. Hydrogen Energy*, **42**, 12122 (2017).
38. C.-I. Wu, J.-W. Huang, Y.-L. Wen, S.-B. Wen, Y.-H. Shen and M.-Y. Yeh, *Mater. Lett*., **62**, 1923 (2008).
39. A. B. Siddique, A. K. Pramanick, S. Chatterjee and M. Ray, *Sci. Rep*., **8**, 1 (2018).
40. M. B. Suwarnkar, R. S. Dhabbe, A. N. Kadam and K. M. Garadkar, *Ceram. Int*., **40**, 5489 (2014).
41. B. H. Stuart, *Infrared spectroscopy: Fundamentals and applications*, John Wiley & Sons (2004).
42. S. Ramezani, M. Ghobadi and B. N. Bideh, *Sensors Actuators B Chem*., **192**, 648 (2014).
43. N. P. Shetti, D. S. Nayak, S. J. Malode and R. M. Kulkarni, *J. Electrochem. Soc*., **164**, B3036 (2016).
44. N. Demir, K. Atacan, M. Ozmen and S. Z. Bas, *New J. Chem*., **44**, 11759 (2020).
45. A. J. Dhulkefl, K. Atacan, S. Z. Bas and M. Ozmen, *Anal. Methods*, **12**, 499 (2020).
46. P. Deng, Z. Xu and J. Li, *Microchim. Acta*., **181**, 1077 (2014).